

# DeepVARwT: Deep Learning for a VAR Model with Trend

Xixi Li<sup>a</sup> and Jingsong Yuan<sup>a</sup>

<sup>a</sup>Department of Mathematics, University of Manchester, UK

## ARTICLE HISTORY

Compiled April 23, 2024

## ABSTRACT

Time series modelling and prediction is useful in many fields of application such as economics, finance and engineering. The vector autoregressive (VAR) model has been used to describe the dependence within and across multiple time series. This is a model for stationary time series, which can be extended to allow the presence of a deterministic trend in each series. In this paper, we demonstrate a new approach that employs deep learning methodology for maximum likelihood estimation of the trend and the dependence structure at the same time. A Long Short-Term Memory (LSTM) network is used for this purpose. We provide a simulation study and applications to real data. In the simulation study, we use realistic trend functions generated from real data and compare the estimates with true function/parameter values. In the real data applications, we compare the prediction performance of this model with state-of-the-art models in the literature.

## KEYWORDS

Dependence modeling, VAR, Causality condition, Trend, Deep learning

## 1. Introduction

In practice, many time series exhibit nonstationary characteristics in the mean. For example, Fig. 1 shows three quarterly US macroeconomic series, namely GDP gap, inflation, and federal funds rate, as analyzed by [13]. Each series is nonstationary as the mean is apparently not constant. More examples of time series with trends will be given in Sections 4.2 and 4.3.

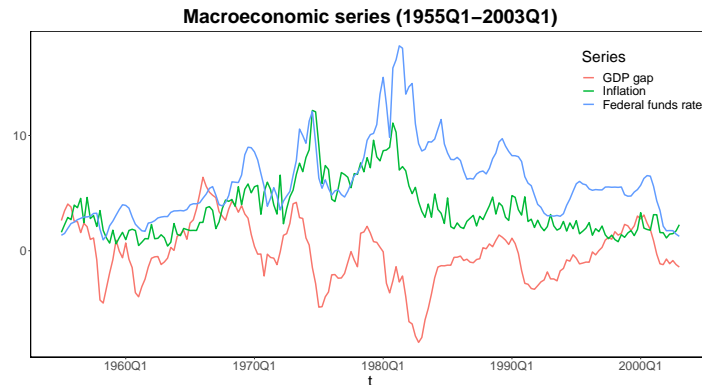


Figure 1. US macroeconomic series spanning 1955Q1 to 2003Q1.

A simple approach to detrending a time series is to difference it until it appears to be stationary. This is effective when the trend is a low order polynomial. However, the trend itself may be of interest, and modeling it together with the dependence structure can be preferable. The former can be estimated by smoothing the data, using methods such as Kernel Smoothing [26], Locally Weighted Scatterplot Smoothing (Lowess), or Smoothing Splines, to name just a few. The series after removing the trend in each component can then be analyzed by fitting a stationary model. Inference on model parameters will have to ignore errors in estimating the trend in this semi-parametric approach in two stages.

The vector autoregressive VAR( $p$ ) model

$$\mathbf{y}_t = A_1\mathbf{y}_{t-1} + A_2\mathbf{y}_{t-2} + \cdots + A_p\mathbf{y}_{t-p} + \boldsymbol{\varepsilon}_t, \quad t = 0, \pm 1, \pm 2, \dots, \quad (1)$$

is for stationary time series  $\{\mathbf{y}_t\}$ , where  $A_1, \dots, A_p$  are constant coefficient matrices, and  $\{\boldsymbol{\varepsilon}_t\}$  is multivariate white noise. It can be extended to accommodate a polynomial trend in each series. If we assume the mean  $\boldsymbol{\mu}_t$  of  $\mathbf{y}_t$  consists of  $k$ -th order polynomials, and  $\{\mathbf{y}_t - \boldsymbol{\mu}_t\}$  satisfies the VAR model (1), then a VAR with trend (VARwT) model can be written as

$$\mathbf{y}_t = A_1\mathbf{y}_{t-1} + A_2\mathbf{y}_{t-2} + \cdots + A_p\mathbf{y}_{t-p} + C\mathbf{x}_t + \boldsymbol{\varepsilon}_t, \quad t = 0, \pm 1, \pm 2, \dots, \quad (2)$$

where  $\mathbf{x}_t = (1, t, t^2, \dots, t^k)'$  and  $C$  is a matrix of constants. Both the trend and the dependence parameters can be estimated simultaneously using ordinary least squares [21].

Fig. 2 shows polynomial trends estimated together with VAR(4) coefficients for the series in Fig. 1. We can see that even with a relatively high order  $k = 9$ , the trend functions missed a few peaks and troughs in the data. In other words, there appears to be over smoothing.

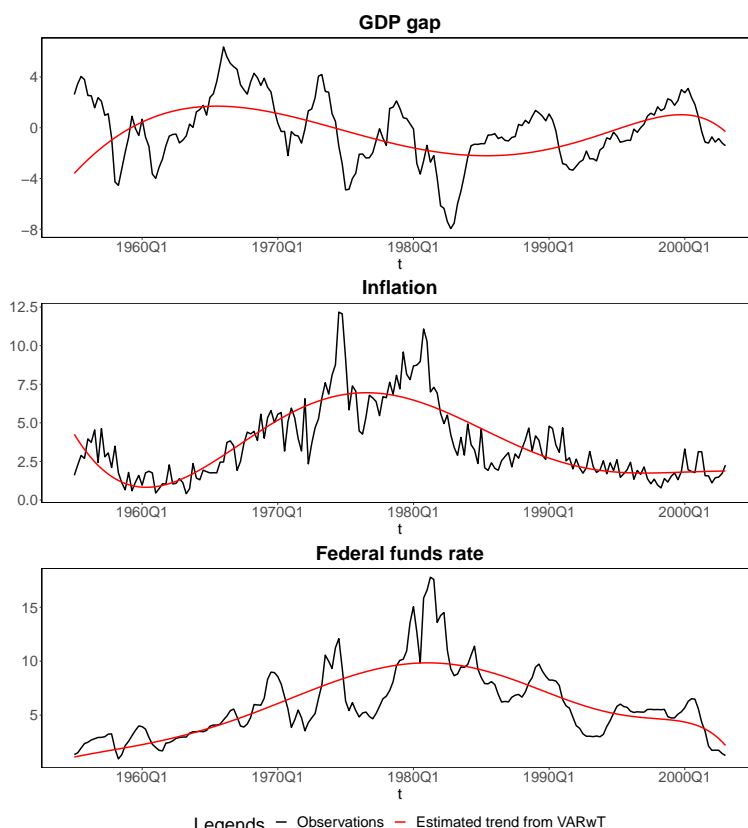


Figure 2. US macroeconomic series and estimated polynomial trends (red lines).

An alternative to fitting polynomial trends is to use B-splines and the results can often get better. A practitioner will face a choice of trend models, while remembering not to ignore dependence in the errors, especially when they have prediction in mind.

Recent advances in machine learning have made available to the statistics community a wealth of network structures and the associated training methodologies for finding patterns in vast quantities of data. There have been attempts at deep learning based statistical forecasting, see [28] [25][23]. All these methods require the time series to be independent so that the loss function can be written in a simple additive form, thus leaving out dependence information across the series.

In this paper, we model the mean  $\mu_t$  by a recurrent neural network of the LSTM (Long Short-Term Memory) type, with input  $x_t$  at time  $t$  to be defined later, and simultaneously  $\{y_t - \mu_t\}$  by the VAR model (1). All the model parameters are estimated at the same time. The exact Gaussian log-likelihood is used, and no assumption is made on the independence between the component series. We enforce the causality condition on the VAR parameters to ensure the stability of the model. This is often overlooked in the literature.

The rest of the paper is organized as follows: Section 2 defines the model and discusses trend generation, VAR parameterization, the Gaussian log-likelihood function, and its use in network training. Section 3 is a simulation study using trends generated from real data. Section 4 shows results of model fitting to three data sets and comparisons with alternative models in terms of forecasting accuracy. Section 5 offers concluding remarks.

## 2. Model fitting and prediction

The Deep VAR with trend (DeepVARwT) model is given by

$$y_t - \mu_t = A_1(y_{t-1} - \mu_{t-1}) + A_2(y_{t-2} - \mu_{t-2}) + \dots + A_p(y_{t-p} - \mu_{t-p}) + \varepsilon_t, \quad t = 0, \pm 1, \pm 2, \dots, \quad (3)$$

where  $\{\varepsilon_t\}$  is i.i.d. Gaussian vector white noise with mean vector  $\mathbf{0}$  and variance-covariance matrix  $\Sigma$ . It is also assumed that as a result of causality,  $\varepsilon_t$  is uncorrelated with  $y_{t-1}, y_{t-2}, \dots$ , so that the RHS of (3) consists of the best linear predictor  $\hat{y}_t - \mu_t$  of  $y_t - \mu_t$  in terms of  $y_{t-1}, y_{t-2}, \dots$  (infinite past) and the prediction error  $\varepsilon_t$ . The trend  $\mu_t$  as well as  $A_1, \dots, A_p$  and  $\Sigma$  will all come from an LSTM network which is described below.

The difference between this model and the VARwT model (2) is in the formulation of  $\mu_t$ . If we leave  $\mu_t$  unspecified, we have a semi-parametric model.

### 2.1. Long Short-Term Memory (LSTM)

A neural network takes input  $x_t$  at time  $t$ , passes it through layers of neurons (processing units) to produce an output. A weighted average of all the input received at each neuron goes into an activation function to produce output for the next stage. A recurrent network also uses output at time  $t - 1$  as input for time  $t$ . An LSTM network has special cells and gates to control information flow. At time  $t$ , the memory cell  $c_t$  puts information from the last memory cell  $c_{t-1}$  through the forget gate  $f_t$  and information from the candidate memory cell  $c_t$  through the input gate  $i_t$ . The output gate  $o_t$  decides how much information from the memory cell  $c_t$  should contribute to the hidden state  $h_t$ . Fig. 3 shows the computation unit for the hidden state  $h_t$  in an LSTM network and the corresponding calculations are as follows [5].

$$\begin{aligned}
\text{Input gate:} & \quad \mathbf{i}_t = \sigma(W_{xi}\mathbf{x}_t + W_{hi}\mathbf{h}_{t-1} + \mathbf{b}_i), \\
\text{Forget gate:} & \quad \mathbf{f}_t = \sigma(W_{xf}\mathbf{x}_t + W_{hf}\mathbf{h}_{t-1} + \mathbf{b}_f), \\
\text{Output gate:} & \quad \mathbf{o}_t = \sigma(W_{xo}\mathbf{x}_t + W_{ho}\mathbf{h}_{t-1} + \mathbf{b}_o), \\
\text{Candidate memory cell:} & \quad \mathbf{c}_t = \tanh(W_{xc}\mathbf{x}_t + W_{hc}\mathbf{h}_{t-1} + \mathbf{b}_c), \\
\text{Memory cell:} & \quad \mathbf{c}_t = \mathbf{f}_t \odot \mathbf{c}_{t-1} + \mathbf{i}_t \odot \mathbf{c}_t, \\
\text{Hidden state:} & \quad \mathbf{h}_t = \mathbf{o}_t \odot \tanh(\mathbf{c}_t),
\end{aligned} \tag{4}$$

where  $W_{xi}$ ,  $W_{xf}$ ,  $W_{xo}$ ,  $W_{hi}$ ,  $W_{hf}$ ,  $W_{ho}$ ,  $W_{xc}$  and  $W_{hc}$  are weight parameters,  $\mathbf{b}_i$ ,  $\mathbf{b}_f$ ,  $\mathbf{b}_o$  and  $\mathbf{b}_c$  are bias parameters,  $\sigma(\cdot)$  is the sigmoid function and the operator  $\odot$  denotes the element-wise product.

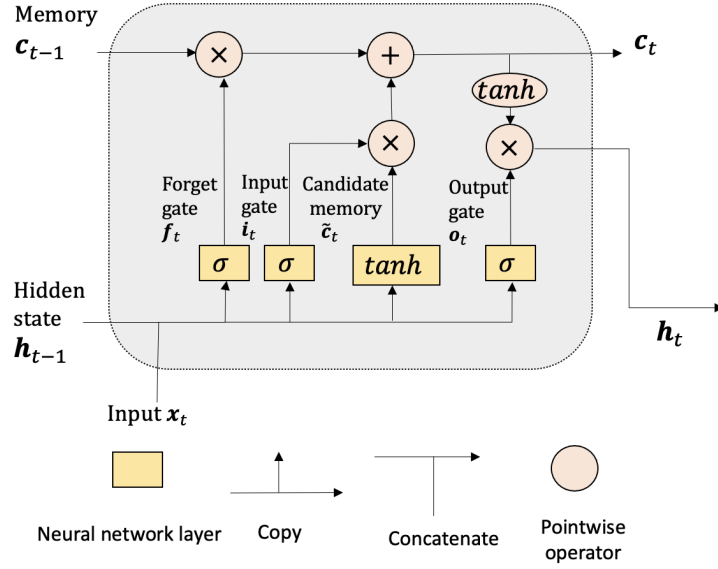


Figure 3. The computation unit for hidden state  $\mathbf{h}_t$  in an LSTM.

## 2.2. Time-dependent trend generation using LSTM

The hidden state

$$\mathbf{h}_t = \text{LSTM}(\mathbf{h}_{t-1}, \mathbf{x}_t; \phi), \tag{5}$$

is mapped to the trend term

$$\boldsymbol{\mu}_t = W_\mu \mathbf{h}_t + \mathbf{b}_\mu, \tag{6}$$

where  $\mathbf{x}_t$  is the input,  $= (t, t^2, t^3)'$  (say, with  $t$  suitably scaled),  $\phi$  contains the weight and bias parameters in (4),  $W_\mu$  and  $\mathbf{b}_\mu$  are additional weight and bias parameters respectively.

## 2.3. VAR parameter generation

Let  $m$  be the dimension of  $\mathbf{y}_t$  and  $p$  the order of the VAR model for  $\{\mathbf{y}_t - \boldsymbol{\mu}_t\}$ . We allocate  $m^2 p$  parameters in the neural network to form candidates for the coefficient matrices  $A_1, \dots, A_p$ , and another  $m(m+1)/2$  parameters to form a lower triangular matrix  $L$ . The latter is used to

construct  $\Sigma = LL'$  for the variance-covariance matrix of  $\varepsilon_t$ . These parameters are initialized and updated by the network together with other network parameters. The candidate coefficient matrices  $A_1, \dots, A_p$  go through the next step of reparameterization.

#### 2.4. Reparameterizing VAR( $p$ ) to enforce causality

It is usually assumed that model (1) is causal in the sense that  $\mathbf{y}_t$  can be expressed linearly in terms of  $\varepsilon_t, \varepsilon_{t-1}, \dots$ , so that  $\varepsilon_t$  is the innovation or one-step-ahead prediction error corresponding to the best linear predictor  $\hat{\mathbf{y}}_t = A_1\mathbf{y}_{t-1} + A_2\mathbf{y}_{t-2} + \dots + A_p\mathbf{y}_{t-p}$  of  $\mathbf{y}_t$  in terms of  $\mathbf{y}_{t-1}, \mathbf{y}_{t-2}, \dots$ . The causality condition is that all the roots of  $\det(I - A_1z - A_2z^2 - \dots - A_pz^p)$  lie outside the unit circle [7]. It also ensures that the linear system given by (1) is stable in the sense that bounded input leads to bounded output.

The parameter space of a causal VAR model is highly complicated. In the univariate case it can be mapped to  $(-1, 1)$  in each dimension using partial autocorrelations, see [2]. Work on the multivariate case include [18], [1], [24] and [9].

Given a set of candidate VAR coefficient matrices  $A_1, \dots, A_p$ , we transform them using the Ansley-Kohn transform [1] in the following two steps, so that the causality condition is satisfied.

- **Partial autocorrelation matrix construction.** For  $j = 1, \dots, p$ , find the Cholesky factorization  $I + A_j A_j' = B_j B_j'$ , then compute

$$P_j = B_j^{-1} A_j \quad (7)$$

as partial autocorrelation matrices [1].

- **Causal VAR coefficient generation.** The partial autocorrelation matrices  $\{P_j\}$  are mapped into the coefficient matrices  $\{A_{s,i}\}$  and  $\{A_{s,i}^*\}$  for forward and backward predictions using  $s$  past/future values, with prediction error variance-covariance matrices  $\Sigma_s$  and  $\Sigma_s^*$  respectively. The answers for  $s = p$  are used to calculate new  $A_1, \dots, A_p$ .

**Initialization:** Make  $\Sigma_0 = \Sigma_0^* = I$ , and  $L_0 = L_0^* = I$ ,  $I$  being the identity matrix.

**Recursion:** For  $s = 0, \dots, p-1$ ,

- Compute

$$A_{s+1,s+1} = L_s P_{s+1} (L_s^*)^{-1}, \quad A_{s+1,s+1}^* = L_s^* P_{s+1}' L_s^{-1}. \quad (8)$$

- For  $i = 1, \dots, s$  ( $s > 0$ ), compute

$$\begin{aligned} A_{s+1,i} &= A_{s,i} - A_{s+1,s+1} A_{s,s-i+1}^* \\ A_{s+1,i}^* &= A_{s,i}^* - A_{s+1,s+1}^* A_{s,s-i+1}. \end{aligned} \quad (9)$$

- Compute

$$\Sigma_{s+1} = \Sigma_s - A_{s+1,s+1} \Sigma_s A_{s+1,s+1}' \quad (10)$$

$$\Sigma_{s+1}^* = \Sigma_s^* - A_{s+1,s+1}^* \Sigma_s^* (A_{s+1,s+1}^*)' \quad (11)$$

and obtain their Cholesky factorizations  $L_{s+1} L_{s+1}'$  and  $L_{s+1}^* L_{s+1}^{*}$  respectively.

**Causal VAR coefficients:** Compute new

$$A_i = (LL_p^{-1})A_{pi}(LL_p^{-1})^{-1}, \quad i = 1, \dots, p \quad (12)$$

to use as casual VAR( $p$ ) coefficient matrices.

## 2.5. The Gaussian log-likelihood

Given that the time series  $\{\mathbf{y}_t\}$  has a Gaussian structure and AR( $p$ ) dependence, the likelihood of  $\mathbf{y} = (\mathbf{y}'_1, \dots, \mathbf{y}'_T)'$  can be written as

$$L(\theta; \mathbf{y}) = f(\mathbf{y}_1, \dots, \mathbf{y}_p) \prod_{t=p+1}^T f(\mathbf{y}_t | \mathbf{y}_{t-1}, \dots, \mathbf{y}_{t-p}), \quad (13)$$

using the joint normal density  $f(\mathbf{y}_1, \dots, \mathbf{y}_p)$  and the conditional Gaussian densities  $f(\mathbf{y}_t | \mathbf{y}_{t-1}, \dots, \mathbf{y}_{t-p})$ ,  $t = p+1, \dots, T$ , where  $\theta$  consists of the parameters  $\psi_1 = \{\phi, W_\mu, \mathbf{b}_\mu\}$  for trend generation and  $\psi_2$  for the VAR coefficient matrices  $A_1, \dots, A_p$  and the  $\Sigma$  matrix. The log-likelihood is

$$\ell(\theta; \mathbf{y}) = -\frac{1}{2} \left[ n \log(2\pi) + \log |R_p| + (\mathbf{y}_{1:p} - \boldsymbol{\mu}_{1:p})' R_p^{-1} (\mathbf{y}_{1:p} - \boldsymbol{\mu}_{1:p}) + (T-p) \log |\Sigma| + \sum_{t=p+1}^T \boldsymbol{\varepsilon}'_t \Sigma^{-1} \boldsymbol{\varepsilon}_t \right], \quad (14)$$

where  $n = mT$  ( $m$  being the dimension of  $\mathbf{y}_t$ ),  $R_p$  is the variance-covariance matrix of  $\mathbf{y}_{1:p} = (\mathbf{y}'_1, \dots, \mathbf{y}'_p)'$  obtained using standard results [17],  $\boldsymbol{\mu}_{p+1}, \dots, \boldsymbol{\mu}_T$  from the output of the neural network and the VAR coefficient matrices  $A_1, \dots, A_p$  are used for the recursive calculation of  $\boldsymbol{\varepsilon}_{p+1}, \dots, \boldsymbol{\varepsilon}_T$  according to (3).

## 2.6. Network training

We employ the popular tool PyTorch [20] for network training, after setting up its structure. The parameters of the neural network are updated by a modified gradient descent (GD) algorithm AdaGrad (Adaptive Gradient) [3]. The basic idea of gradient descent is to follow the opposite direction of the gradient of the loss function at the current point. Compared with conventional gradient descent algorithms, AdaGrad provides individual adaptive learning rates for different parameters. At iteration  $k$ , the learning rate is modified by the diagonal elements of  $G = \sum_{\tau=1}^k \mathbf{g}^{(\tau)} \mathbf{g}^{(\tau) \prime}$ , where  $\mathbf{g}^{(\tau)}$  is the gradient of the loss function at iteration  $\tau$ .

Details of the GD based training procedure are presented in Algorithm 1, where the initial values  $\psi_1^{(0)}$  for the trend part are obtained by minimising the sum of squares of differences between  $\mathbf{y}_t$  and  $\boldsymbol{\mu}_t$  (nonlinear least squares), and  $\psi_2^{(0)} = \{A_1^{(0)}, \dots, A_p^{(0)}, L^{(0)}\}$  by fitting VAR( $p$ ) to the detrended data using OLS and Cholesky factorization. The initial state  $\mathbf{h}_0$  and the initial candidate memory cell  $\mathbf{c}_0$  are both set to  $\mathbf{0}$ . The loss function then becomes minus the log-likelihood for network training. The trend parameters are fine-tuned with a smaller learning rate so that the trend terms get updated in small steps to avoid large changes that affect the estimation of the VAR parameters.

---

**Algorithm 1** GD based network training for VAR with trend

---

**Input:**

- Time series observations  $\mathbf{y}_1, \dots, \mathbf{y}_T$ ;
- Values of input to the network  $\mathbf{x}_1, \dots, \mathbf{x}_T$ ;
- Learning rates  $\eta_1$  and  $\eta_2$ ;
- Number of iterations  $K$ ;
- Precision value  $prec$  for the stopping criteria.

**Output:**

Optimal network parameter values  $(\boldsymbol{\psi}_1^{(k)}, \boldsymbol{\psi}_2^{(k)})$ .

- 1: Set  $k = 0, rc_1 = rc_2 = prec + 1$ .
  - 2: **while**  $k \leq K$  and  $(rc_1 > prec$  or  $rc_2 > prec)$  **do** ▶ Iterations for MLE/network optimization.
  - 3:   **for**  $t \leftarrow 1$  to  $T$  **do**
  - 4:     Compute hidden state  $\mathbf{h}_t^{(k)} = \text{LSTM}(\mathbf{h}_{t-1}^{(k)}, \mathbf{x}_t; \boldsymbol{\phi}^{(k)})$ .
  - 5:     Compute trend term  $\boldsymbol{\mu}_t^{(k)} = W_\mu^{(k)} \mathbf{h}_t^{(k)} + \mathbf{b}_\mu^{(k)}$ .
  - 6:   **end for**
  - 7:   Compute  $P_1^{(k)}, \dots, P_p^{(k)}$  from  $A_1^{(k)}, \dots, A_p^{(k)}$  using (7).
  - 8:   Transform  $P_1^{(k)}, \dots, P_p^{(k)}$  into new  $A_1^{(k)}, \dots, A_p^{(k)}$  using (8) to (12).
  - 9:   Compute  $\Sigma^{(k)} = L^{(k)} L^{(k)'}$ .
  - 10:   Evaluate loss function  $-\ell(\boldsymbol{\theta}^{(k)}; \mathbf{y})$  at  $\boldsymbol{\theta}^{(k)} = (\boldsymbol{\psi}_1^{(k)}, \boldsymbol{\psi}_2^{(k)})$  using (14).
  - 11:   Compute relative change of log-likelihood ( $k \geq 2$ ):  
    
$$rc_1 = \left| \frac{\ell(\boldsymbol{\theta}^{(k-1)}; \mathbf{y}) - \ell(\boldsymbol{\theta}^{(k-2)}; \mathbf{y})}{\ell(\boldsymbol{\theta}^{(k-2)}; \mathbf{y})} \right|.$$
  - 12:   Compute relative change of log-likelihood ( $k \geq 1$ ):  
    
$$rc_2 = \left| \frac{\ell(\boldsymbol{\theta}^{(k)}; \mathbf{y}) - \ell(\boldsymbol{\theta}^{(k-1)}; \mathbf{y})}{\ell(\boldsymbol{\theta}^{(k-1)}; \mathbf{y})} \right|.$$
  - 13:   Compute gradient of loss function  
    
$$\mathbf{g}_1^{(k)} = \left. \frac{\partial}{\partial \boldsymbol{\psi}_1} (-\ell(\boldsymbol{\theta}; \mathbf{y})) \right|_{\boldsymbol{\theta}=\boldsymbol{\theta}^{(k)}}, \mathbf{g}_2^{(k)} = \left. \frac{\partial}{\partial \boldsymbol{\psi}_2} (-\ell(\boldsymbol{\theta}; \mathbf{y})) \right|_{\boldsymbol{\theta}=\boldsymbol{\theta}^{(k)}}.$$
  - 14:   Compute  $G_1 = \sum_{\tau=0}^k \mathbf{g}_1^{(\tau)} \mathbf{g}_1^{(\tau)'}$ ,  $G_2 = \sum_{\tau=0}^k \mathbf{g}_2^{(\tau)} \mathbf{g}_2^{(\tau)'}$ .
  - 15:   Update trend parameters  $\boldsymbol{\psi}_1^{(k+1)} = \boldsymbol{\psi}_1^{(k)} - \eta_1 \text{diag}(G_1)^{-\frac{1}{2}} \odot \mathbf{g}_1^{(k)}$ .
  - 16:   Update VAR parameters  $\boldsymbol{\psi}_2^{(k+1)} = \boldsymbol{\psi}_2^{(k)} - \eta_2 \text{diag}(G_2)^{-\frac{1}{2}} \odot \mathbf{g}_2^{(k)}$ .
  - 17:    $k \leftarrow k + 1$
  - 18: **end while**
- 

## 2.7. Prediction from trained network

We continue to run the trained network for  $t = T + 1, T + 2$  etc to generate future trend values  $\boldsymbol{\mu}_t$  and produce point forecasts using the formula (A9) in the Appendix.

Approximate 95% prediction intervals can be obtained by adding or subtracting 1.96 times the standard deviations of prediction errors using results in the Appendix.

### 3. Simulation study

To assess the finite sample performance of the deep learning based maximum likelihood estimation method, we simulated 100 samples each of size  $T = 800$  from the semi-parametric VAR(2) model

$$\mathbf{y}_t - \boldsymbol{\mu}_t = A_1(\mathbf{y}_{t-1} - \boldsymbol{\mu}_{t-1}) + A_2(\mathbf{y}_{t-2} - \boldsymbol{\mu}_{t-2}) + \boldsymbol{\varepsilon}_t, \quad (15)$$

where

$$A_1 = \begin{pmatrix} -1.0842 & -0.1245 & 0.3137 \\ -0.7008 & -0.3754 & -0.2064 \\ 0.3166 & 0.3251 & 0.2135 \end{pmatrix}, \quad A_2 = \begin{pmatrix} -0.5449 & -0.3052 & -0.1952 \\ -0.4057 & 0.5129 & 0.3655 \\ 0.0054 & -0.2911 & 0.2066 \end{pmatrix},$$

and

$$\Sigma = \begin{pmatrix} 0.4834 & -0.2707 & 0.1368 \\ -0.2707 & 0.4079 & -0.0221 \\ 0.1368 & -0.0221 & 0.4103 \end{pmatrix}$$

is the variance-covariance matrix of  $\boldsymbol{\varepsilon}_t$ . Values of the trend term  $\boldsymbol{\mu}_t$  were obtained by kernel smoothing from daily closing prices of three US stocks from 3rd October 2016 to 5th December 2019.

An example of the simulated multiple series is shown in Fig. 4, each having clearly a trend that looks more realistic than artificial functions.

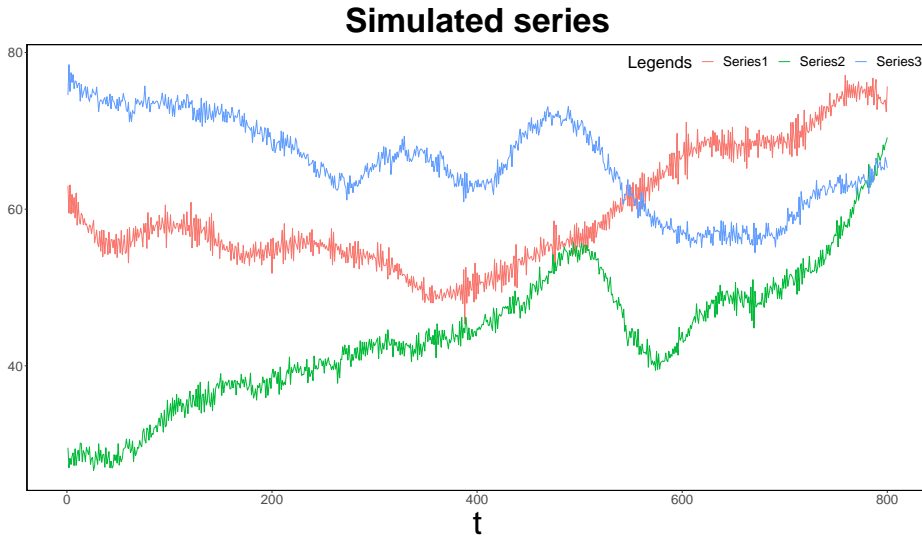


Figure 4. Simulated series from VAR(2) model with trend.

We used an LSTM network with one hidden layer of 20 units. The input at time  $t$  was  $\mathbf{x}_t = (t, t^2, t^3, 1/t, 1/t^2, 1/t^3)'$ . The learning rates were  $\eta_1 = 0.001$  and  $\eta_2 = 0.01$ , with  $K = 600$  iterations and precision  $prec = 10^{-5}$ . The computation time for each set of parameter estimates was about 1 hour on an Intel Core i9 2.3 GHz processor with eight cores.



### 3.1. Simulation results

Following [4], we use mean absolute deviation

$$\text{MAD}_i = \frac{1}{3 \times 800} \sum_{k=1}^3 \sum_{t=1}^{800} |\hat{\mu}_{kt}^{(i)} - \mu_{kt}|$$

to evaluate the accuracy of trend estimation in the  $i$ th simulation run,  $i = 1, \dots, 100$ . Fig. 5 shows estimated trends from DeepVARwT (left panel) and VARwT (right panel) with MAD at the first quartile (short dashed, black), the median (dotted, red), and the third quartile (long dashed, black) respectively among the 100 simulation runs. The estimated trends from our model follow the true trends very closely while those from VARwT show over-smoothing of local changes.

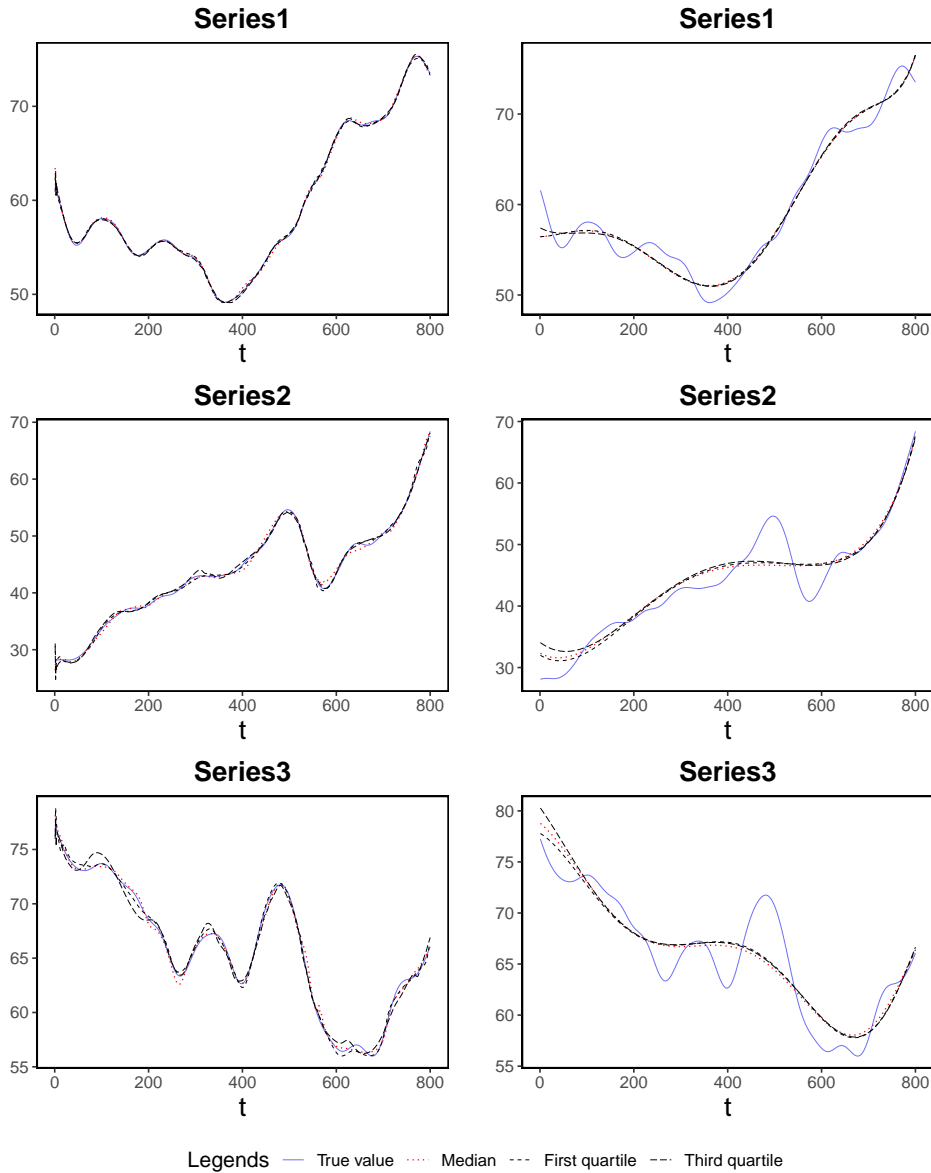


**Figure 5.** True (solid, blue) and estimated trends from DeepVARwT (left pane) and VARwT (right pane) with MAD at first quartile (short dashed, black), third quartile (long dashed, black), and median (dotted, red).

Table 1 reports summary statistics of 100 estimates of each parameter from our model and VARwT, where  $a_{jk}^{(i)}$  refers to the  $(j, k)$ -th entry of the coefficient matrix  $A_i$  and  $\sigma_{jk}$  is the  $(j, k)$ -th entry of the variance-covariance matrix  $\Sigma$ . We can observe that compared with VARwT, the DeepVARwT model gives rise to reduced biases at the expense of standard deviations (SDs). The parameter estimates are more accurate with smaller mean squared errors (MSEs) than those obtained from the VARwT model.

**Table 1.** Estimation results of DeepVARwT and VARwT: true value above sample mean, standard deviation, mean squared error of 100 estimates of each parameter and sample bias.

True value	$a_{11}^{(1)}$	$a_{12}^{(1)}$	$a_{13}^{(1)}$	$a_{21}^{(1)}$	$a_{22}^{(1)}$	$a_{23}^{(1)}$	$a_{31}^{(1)}$	$a_{32}^{(1)}$	$a_{33}^{(1)}$
	-1.0842	-0.1245	0.3137	-0.7008	-0.3754	-0.2064	0.3166	0.3251	0.2135
DeepVARwT									
Mean	-1.0103	-0.1199	0.2671	-0.6802	-0.3410	-0.2240	0.2900	0.3601	0.2891
Bias	0.0739	0.0046	-0.0466	0.0206	0.0344	-0.0176	-0.0266	0.035	0.0756
SD	0.1776	0.0816	0.0861	0.0784	0.0813	0.0622	0.0421	0.0465	0.0945
MSE	0.0367	0.0066	0.0095	0.0065	0.0077	0.0041	0.0025	0.0034	0.0146
VARwT									
Mean	0.0133	0.3386	0.0185	-0.2269	0.1029	-0.4148	0.1871	0.3508	0.5027
Bias	1.0975	0.4631	-0.2952	0.4739	0.4783	-0.2084	-0.1295	0.0257	0.2892
SD	0.0179	0.0457	0.0417	0.0178	0.0266	0.0239	0.0128	0.0187	0.0228
MSE	1.2047	0.2166	0.0889	0.2249	0.2295	0.0440	0.0169	0.0010	0.0841
DeepVARwT									
True value	$a_{11}^{(2)}$	$a_{12}^{(2)}$	$a_{13}^{(2)}$	$a_{21}^{(2)}$	$a_{22}^{(2)}$	$a_{23}^{(2)}$	$a_{31}^{(2)}$	$a_{32}^{(2)}$	$a_{33}^{(2)}$
	-0.5449	-0.3052	-0.1952	-0.4057	0.5129	0.3655	0.0054	-0.2911	0.2066
DeepVARwT									
Mean	-0.4674	-0.3246	-0.2213	-0.3677	0.5431	0.3756	-0.0245	-0.2643	0.2692
Bias	0.0775	-0.0194	-0.0261	0.038	0.0302	0.0101	-0.0299	0.0268	0.0626
SD	0.2086	0.0645	0.0528	0.1039	0.0801	0.0460	0.0566	0.0368	0.0833
MSE	0.0499	0.0045	0.0034	0.0121	0.0073	0.0022	0.0041	0.0021	0.0108
VARwT									
Mean	0.7127	-0.2808	-0.1122	0.2335	0.8189	0.4848	-0.1662	-0.2880	0.3966
Bias	1.2576	0.0244	0.0830	0.6392	0.3060	0.1193	-0.1716	0.0031	0.1900
SD	0.0206	0.0468	0.0435	0.0186	0.0280	0.0231	0.0127	0.0177	0.0233
MSE	1.5820	0.0028	0.0088	0.4089	0.0944	0.0148	0.0296	0.0003	0.0366
DeepVARwT									
True value	$\sigma_{11}$	$\sigma_{21}$	$\sigma_{22}$	$\sigma_{31}$	$\sigma_{32}$	$\sigma_{33}$			
	0.4834	-0.2707	0.4079	0.1368	-0.0221	0.4103			
DeepVARwT									
Mean	0.5357	-0.2652	0.4283	0.1175	-0.0285	0.4347			
Bias	0.0523	0.0055	0.0204	-0.0193	-0.0064	0.0244			
SD	0.1321	0.0597	0.0575	0.0275	0.0196	0.0424			
MSE	0.0200	0.0036	0.0037	0.0011	0.0004	0.0024			
VARwT									
Mean	1.2291	-0.0039	0.6636	0.0714	-0.0625	0.5114			
Bias	0.7457	0.2668	0.2557	-0.0654	-0.0404	0.1011			
SD	0.0811	0.0267	0.0352	0.0312	0.0206	0.0265			
MSE	0.5626	0.0719	0.0666	0.0052	0.0020	0.0109			

## 4. Real data applications

### 4.1. US macroeconomics series 1

For the US macroeconomic series (Fig. 1), we fit a model and make forecasts 20 times, each time using a training sample of size  $T = 166$ . The training samples are  $y_{1:T}^{(i)} = \{y_i, y_{i+1}, \dots, y_{i+T-1}\}$ ,  $i = 1, \dots, 20$ , and we forecast  $h = 1, 2, \dots, 8$  quarters ahead.

The order  $p = 4$  for a VAR model is a common choice in the analysis of quarterly macroeconomic series, for example, [14], [15] and [10]. The first model we fitted was DeepVARwT(4). The number of input  $t$  functions and the hidden state size were the two most crucial hyperparameters. A grid search was conducted to find a set of values with maximum likelihood, among 2, 3 or 4  $t$  functions and 5, 10 or 15 hidden states. For efficiency, we relied on our experience to set values for the other hyperparameters. The learning rates were  $\eta_1 = 0.0005$  and  $\eta_2 = 0.01$ , with  $K = 500$  iterations and precision  $prec = 10^{-7}$ .

The estimated trends (red) are shown in Fig. 6 for the first training sample ( $i = 1$ ), which can be seen to follow the observations (black) smoothly.

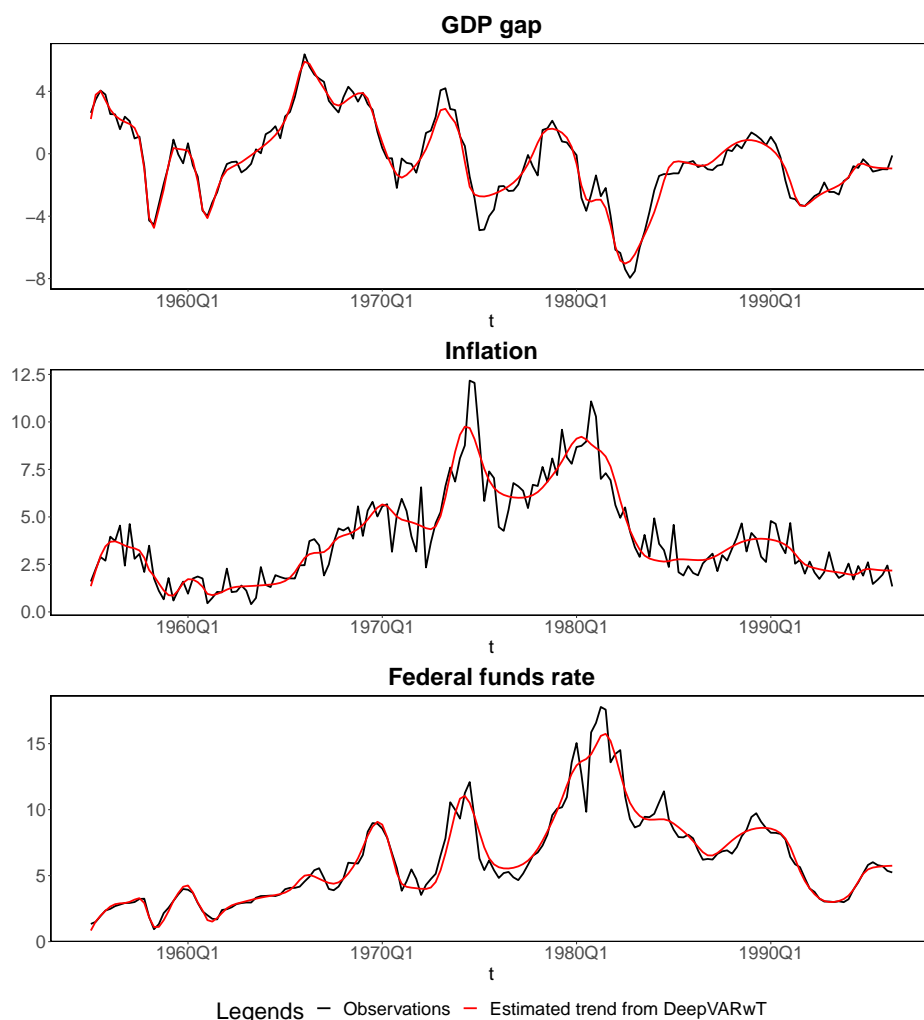


Figure 6. The first training sample (black lines) from 1955Q1 to 1996Q2 and the corresponding estimated trends (red lines).

The sample autocorrelations of residuals are shown in Fig. 7. The results are good for the GDP gap series, reasonable for the federal funds rate series, and a little concerning for the inflation series in terms of the number of values outside the boundaries.

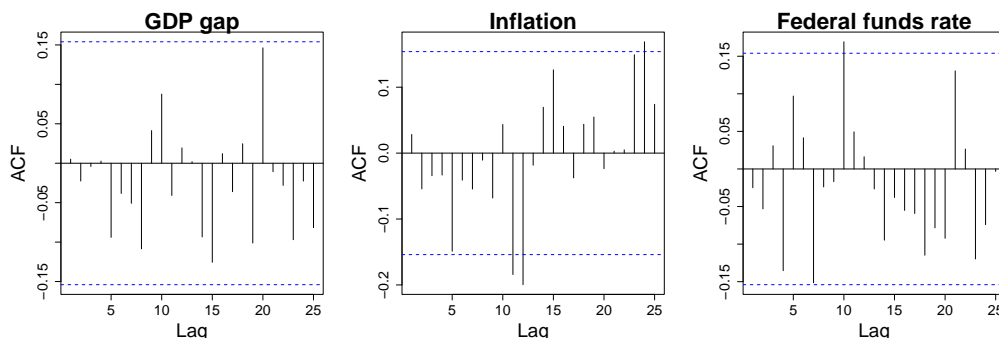


Figure 7. Sample autocorrelations of residuals.

Fig. 8 contains normal QQ plots of the residuals. There is slight deviation from normality for all the series at both ends.

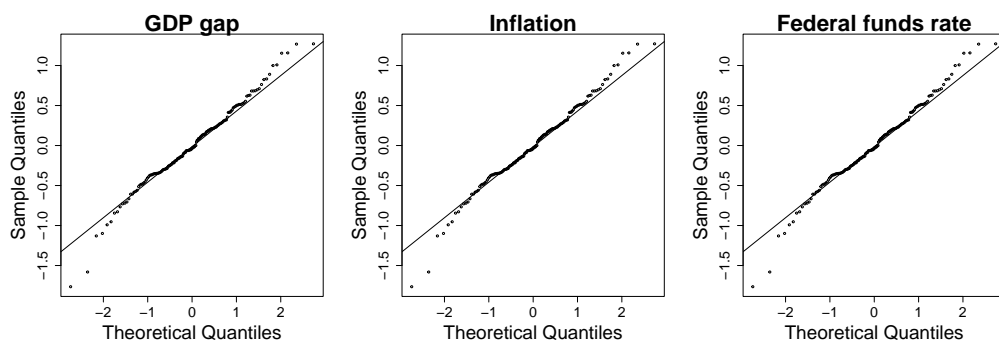


Figure 8. Normal QQ plots of residuals.

For comparison, we also fitted a VARwT(4) model, a DeepAR and a DeepState model using default hyperparameter values. The input at time  $t$  was  $\mathbf{x}_t = (t, t^2, t^3, t^4, t^5, t^6, t^7, t^8, t^9)'$  for the VARwT model to account for the number of turning points in the trend. Table 2 gives a summary of these models and the software packages used.

Table 2. Models used for comparison.

Model	Description	Available software
VARwT	Vector autoregressive model with trend [21]	<code>vars::VAR(exogen=x)</code>
DeepAR	Deep learning based autoregressive model [25]	<code>gluonts.DeepAREstimator()</code>
DeepState	Deep learning based state space model [23]	<code>gluonts.DeepStateEstimator()</code>

To evaluate the accuracy of point forecasts, we computed the  $h$ -step-ahead Absolute Percentage Error averaged over 20 forecasts

$$\text{APE}(h) = \frac{1}{20} \sum_{i=1}^{20} \left| \frac{y_{T+h}^{(i)} - \hat{y}_{T+h}^{(i)}}{y_{T+h}^{(i)}} \right| \times 100$$

for each component series  $\{y_t^{(i)}\}$  in the  $i$ th training sample, where  $\hat{y}_{T+h}^{(i)}$  is the  $h$ -step-ahead

forecast of  $y_{T+h}^{(i)}$ . The Scaled Interval Score [6] is averaged as follows:

$$\text{SIS}(h) = \frac{1}{20} \sum_{i=1}^{20} \frac{(u_{T+h}^{(i)} - l_{T+h}^{(i)}) + \frac{2}{\alpha} (l_{T+h}^{(i)} - y_{T+h}^{(i)}) \mathbb{1}_{\{y_{T+h}^{(i)} < l_{T+h}^{(i)}\}} + \frac{2}{\alpha} (y_{T+h}^{(i)} - u_{T+h}^{(i)}) \mathbb{1}_{\{y_{T+h}^{(i)} > u_{T+h}^{(i)}\}}}{\frac{1}{T-s} \sum_{t=s+1}^T |y_t^{(i)} - y_{t-s}^{(i)}|},$$

to measure the overall accuracy of the  $(1 - \alpha) \times 100\%$  prediction intervals  $(l_{T+h}^{(i)}, u_{T+h}^{(i)})$  for the  $i$ th training sample,  $i = 1, \dots, 20$ , where  $\mathbb{1}_A$  is the indicator function for the condition  $A$ ,  $s$  is the seasonality of the time series ( $s = 4$  for quarterly data).

Table 5 shows the forecasting performances of different models at several horizons  $h = 1, 2, 4, 8$  and averages over  $h = 1, \dots, 4$  and  $h = 1, \dots, 8$ . When a model performs best, the corresponding number in the table will be bold.

- **DeepVARwT vs VARwT.** Compared with VARwT, DeepVARwT produced superior point forecasts at almost all the forecasting horizons for all the series (except  $h = 1$  for GDP gap and  $h = 1, 2$  for inflation). Our model also gave more accurate prediction intervals in the long term ( $h = 4, 8$ ) and overall ( $h = 1 : 4$  and  $h = 1 : 6$ ) for all the series.
- **DeepVARwT vs other deep learning based models.** Compared with DeepAR and DeepState, our model resulted in better point forecasts and prediction intervals at all the forecasting horizons for federal funds rate. It also gave more precise prediction intervals at all the forecasting horizons for GDP gap.

**Table 3.** Performance of DeepVARwT against other models according to APE and SIS.

GDP gap												
	Absolute Percentage Error						Scaled Interval Score					
	$h=1$	$h=2$	$h=4$	$h=8$	$h=1:4$	$h=1:8$	$h=1$	$h=2$	$h=4$	$h=8$	$h=1:4$	$h=1:8$
VARwT	665.927	2982.609	293.199	1124.228	1042.088	897.853	<b>1.592</b>	<b>4.114</b>	34.332	244.788	13.157	81.907
DeepAR	<b>333.063</b>	<b>389.993</b>	173.499	260.860	<b>258.932</b>	<b>240.882</b>	8.280	15.304	35.105	65.816	21.020	39.587
DeepState	1023.302	1070.784	178.982	<b>200.245</b>	612.331	403.614	7.903	16.995	22.545	34.583	16.800	24.950
DeepVARwT	671.569	877.267	<b>162.329</b>	202.388	466.350	326.924	4.847	8.961	<b>14.509</b>	<b>29.158</b>	<b>10.201</b>	<b>17.008</b>
Inflation												
	Absolute Percentage Error						Scaled Interval Score					
	$h=1$	$h=2$	$h=4$	$h=8$	$h=1:4$	$h=1:8$	$h=1$	$h=2$	$h=4$	$h=8$	$h=1:4$	$h=1:8$
VARwT	37.579	55.549	111.768	348.255	69.868	159.859	<b>3.259</b>	<b>6.236</b>	18.767	106.686	9.367	37.482
DeepAR	<b>26.660</b>	<b>32.112</b>	<b>39.840</b>	53.661	<b>34.573</b>	<b>45.584</b>	8.641	8.754	10.845	16.925	9.139	12.297
DeepState	75.164	68.626	75.062	59.455	73.611	69.405	4.553	6.423	<b>3.940</b>	5.121	<b>5.317</b>	6.552
DeepVARwT	66.759	67.948	57.351	<b>46.978</b>	62.079	58.585	8.711	8.727	4.912	<b>4.558</b>	6.701	<b>6.354</b>
Federal funds rate												
	Absolute Percentage Error						Scaled Interval Score					
	$h=1$	$h=2$	$h=4$	$h=8$	$h=1:4$	$h=1:8$	$h=1$	$h=2$	$h=4$	$h=8$	$h=1:4$	$h=1:8$
VARwT	10.521	25.868	90.407	424.838	44.681	157.662	2.226	7.145	31.160	137.790	14.374	53.498
DeepAR	9.685	19.915	55.689	119.189	30.633	62.829	4.759	11.914	33.627	53.807	18.122	32.993
DeepState	33.190	36.782	59.985	128.743	44.186	70.322	6.962	10.260	13.669	22.901	10.862	15.458
DeepVARwT	<b>7.834</b>	<b>14.032</b>	<b>33.676</b>	<b>80.449</b>	<b>19.659</b>	<b>39.916</b>	<b>1.473</b>	<b>3.946</b>	<b>8.805</b>	<b>17.381</b>	<b>5.262</b>	<b>9.541</b>

The DeepVARwT model outperformed the other models for federal funds rate. It gave the best prediction intervals for GDP gap over  $h=1:4$  and  $h=1:8$ , while in second place for prediction accuracy. Its performance is similar for inflation with a slight drop to second place in terms of SIS over  $h=1:4$ .

All the experiments were conducted on an Intel Core i9 2.3 GHz processor with eight cores. The number of weight parameters in the LSTM network for the 20 fitted DeepVARwT models ranged from 715 to 1350. The computation time of 20 predictions from VARwT, DeepAR, DeepState and DeepVARwT was approximately 1, 42, 210, and 55 minutes, respectively.

## 4.2. Global temperatures

Global warming has attracted significant attention in recent research, as demonstrated by studies such as [8], [12], and [11]. Fig. 9 shows three annual temperature anomaly series from distinct regions: the Northern Hemisphere, the Southern Hemisphere and the Tropics from 1850 to 2021, which are described in detail in [19]. The data are temperature anomalies relative to a reference period of 1961-1990 [19]. Each series consists of 172 yearly observations.

From Fig. 9, we can observe obvious trends in the three series. [11] assumed that the trends in the Northern and Southern Hemispheres series are deterministic and modelled the local changes in data using a vector shifting-mean autoregressive model with order  $p = 3$ . We continue to fit a DeepVARwT(3) model to the three series and make predictions  $h = 1, 2, \dots, 6$  steps ahead of  $T = 147$ . As with our first real data application, this is repeated 19 times, each time moving the training sample forward by one time point. The search ranges for the number of  $t$  functions and hidden state size were 2, 3, 4 and 3, 5, 8, respectively. The learning rates were  $\eta_1 = 0.0005$  and  $\eta_2 = 0.01$ , with  $K = 500$  iterations and precision  $prec = 10^{-7}$ .

The forecasts will be compared with those from VARwT(3), DeepAR, and DeepState models with default hyperparameters. The exogenous variables for VARwT are  $\mathbf{x}_t = (t, t^2, t^3, t^4, t^5)'$  to account for the number of turning points in the series.

From Fig. 10, we can see that the estimated trends (red) for the first training sample ( $i = 1$ ) follow the observations (black) smoothly.

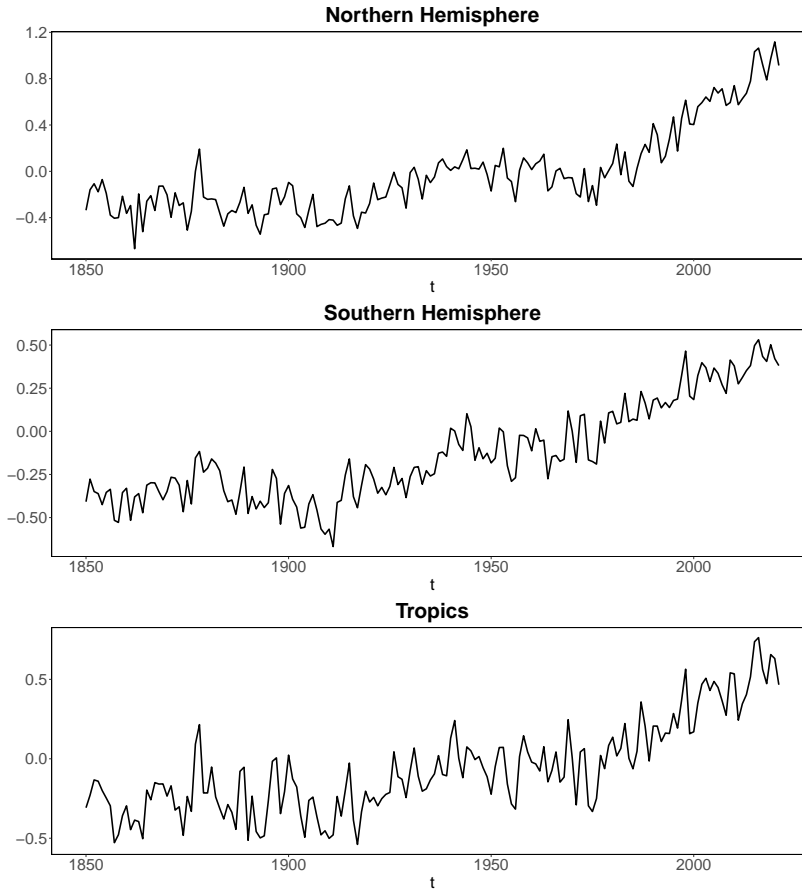


**Figure 9.** Temperature anomaly series for the Northern Hemisphere, the Southern Hemisphere and the Tropics from 1850 to 2021.

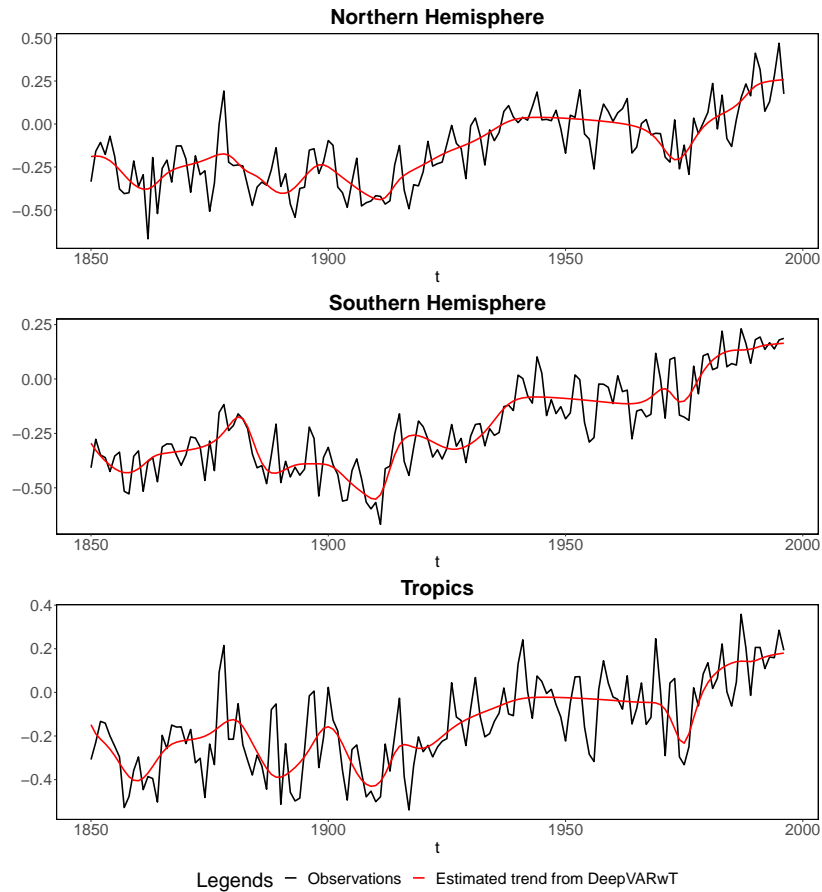


Figure 10. The first training sample (black lines) from 1850 to 1996 and the corresponding estimated trends (red lines).

The sample autocorrelations of residuals are shown in Fig. 11. The results are very good for all the series with all the values within boundaries.

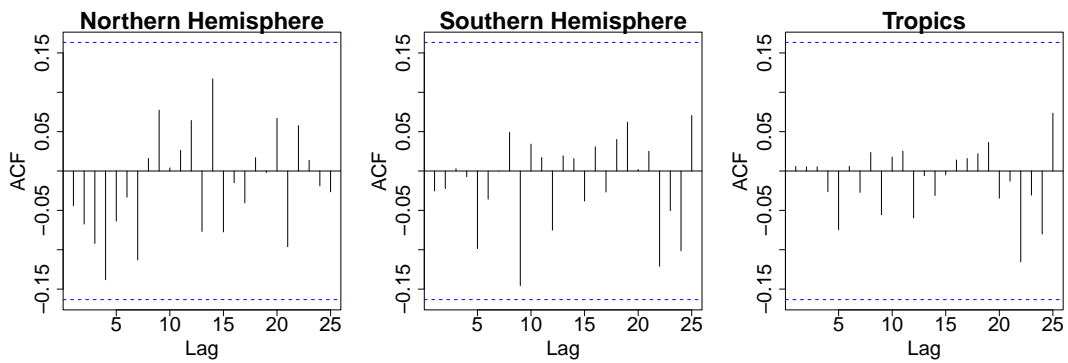


Figure 11. Sample autocorrelations of residuals.

Fig. 12 contains normal QQ plots of the residuals. The results are very good for all the series showing clearly straight line patterns.

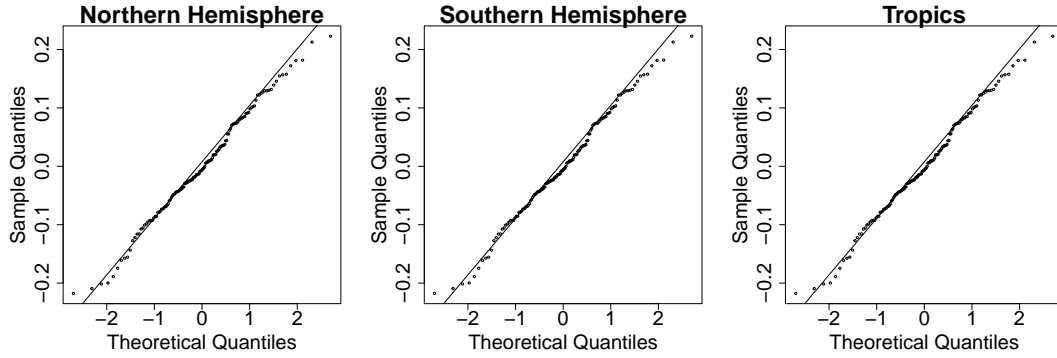


Figure 12. Normal QQ plots of residuals.

Table 4 shows the APE and SIS values of different models at several horizons  $h = 1, 2, 4, 6$  and averaged over  $h = 1 : 3$  and  $h = 1 : 6$ .

- **DeepVARwT vs VARwT.** Compared with the time-invariant VAR with trend, our model produced better point forecasts at all forecasting horizons for all the series. It gave better prediction intervals in the long term ( $h = 4, 6$ ) and overall ( $h = 1 : 6$ ) for all the series.
- **DeepTVARwT vs other deep learning based models.** Compared with DeepAR and DeepState, our model produced more accurate point forecasts at almost all forecasting horizons for all the series (except  $h = 4$  for Tropics). Our model resulted in better prediction intervals at all forecasting horizons for all the series.

Table 4. Performance of DeepVARwT against other models according to APE and SIS.

	Northern Hemisphere											
	Absolute Percentage Error						Scaled Interval Score					
	$h=1$	$h=2$	$h=4$	$h=6$	$h=1:3$	$h=1:6$	$h=1$	$h=2$	$h=4$	$h=6$	$h=1:3$	$h=1:6$
VARwT	26.718	41.661	52.713	67.507	39.222	49.277	8.385	17.526	41.703	75.358	18.991	38.609
DeepAR	25.485	31.243	37.544	44.097	28.563	34.805	30.180	36.423	46.395	58.301	33.411	43.010
DeepState	21.557	30.886	28.141	32.782	27.221	28.245	20.504	35.893	39.854	50.512	32.649	38.265
DeepVARwT	<b>16.852</b>	<b>21.448</b>	<b>19.162</b>	<b>25.364</b>	<b>19.880</b>	<b>21.171</b>	<b>6.955</b>	<b>17.079</b>	<b>14.377</b>	<b>22.310</b>	<b>14.011</b>	<b>15.655</b>
	Southern Hemisphere											
	Absolute Percentage Error						Scaled Interval Score					
	$h=1$	$h=2$	$h=4$	$h=6$	$h=1:3$	$h=1:6$	$h=1$	$h=2$	$h=4$	$h=6$	$h=1:3$	$h=1:6$
VARwT	33.082	47.766	57.959	73.987	45.437	55.317	<b>6.252</b>	<b>9.717</b>	14.918	40.835	9.313	18.502
DeepAR	39.625	43.267	44.622	58.828	38.624	45.408	29.747	32.777	29.830	45.400	28.400	32.624
DeepState	28.808	43.194	26.155	36.493	35.616	33.763	25.584	40.584	24.544	36.837	33.595	32.383
DeepVARwT	<b>23.284</b>	<b>24.090</b>	<b>23.021</b>	<b>31.329</b>	<b>22.696</b>	<b>25.417</b>	6.517	11.101	<b>6.842</b>	<b>8.494</b>	<b>8.401</b>	<b>8.132</b>
	Tropics											
	Absolute Percentage Error						Mean Scaled Interval Score					
	$h=1$	$h=2$	$h=4$	$h=6$	$h=1:3$	$h=1:6$	$h=1$	$h=2$	$h=4$	$h=6$	$h=1:3$	$h=1:6$
VARwT	44.422	62.163	69.043	79.502	58.570	65.516	6.140	<b>9.145</b>	14.144	33.223	<b>8.718</b>	15.790
DeepAR	52.113	48.542	46.185	60.936	46.192	50.176	40.178	34.033	31.429	39.313	31.952	33.657
DeepState	42.780	56.903	<b>29.020</b>	43.003	47.920	41.989	28.412	47.049	26.966	39.685	38.220	35.555
DeepVARwT	<b>30.207</b>	<b>41.150</b>	29.757	<b>34.308</b>	<b>36.679</b>	<b>34.288</b>	<b>4.986</b>	13.592	<b>8.959</b>	<b>10.058</b>	9.948	<b>9.506</b>

Overall, the DeepVARwT model gave better forecasts and prediction intervals than other models, especially for the Northern and Southern Hemisphere series.

The number of weight parameters in the network for the 20 fitted DeepVARwT models varied between 444 and 508. The computation time for generating 20 predictions using VARwT, DeepAR, DeepState and DeepVARwT was about 1, 45, 80, and 30 minutes, respectively.



### 4.3. US macroeconomics series 2

We continue to apply our model to another set of US macroeconomic data (Fig.13) including inflation rate (year-over-year log growth rate of the GDP price index), unemployment rate and treasury interest rate from 1953Q1 to 2001Q3, as analysed by [22]. The inflation rate differs from the first real data example where it is defined as “the percentage change in the GDP, chain-weighted price index at annual rate” [13]. Each series consists of 195 observations and exhibits a clear trend. We fitted a DeepVARwT(4) model to these series and forecast  $h = 1, 2, \dots, 8$  steps ahead of  $T = 168$ . Consistent with our previous real data applications, we repeated 19 times, each time moving the training sample forward by one time point.

The search ranges for the number of  $t$  functions and hidden state size were 2, 3, 4 and 10, 12, 15, respectively. We employed the learning rates  $\eta_1 = 0.0005$  and  $\eta_2 = 0.01$ , with  $K = 500$  iterations and precision  $prec = 10^{-7}$ . The number of weight parameters in the network for the 20 fitted DeepVARwT models varied between 635 and 2,185.

The forecasts will be compared with those from a VARwT(4) model using  $\mathbf{x}_t = (t, t^2, t^3, t^4, t^5, t^6, t^7, t^8, t^9)'$  to account for the number of turning points in the series, DeepAR, [25], and DeepState models with default hyperparameters. The computation time to generate 20 predictions using VARwT, DeepAR, DeepState and DeepVARwT was about 1, 45, 80, and 35 minutes, respectively.

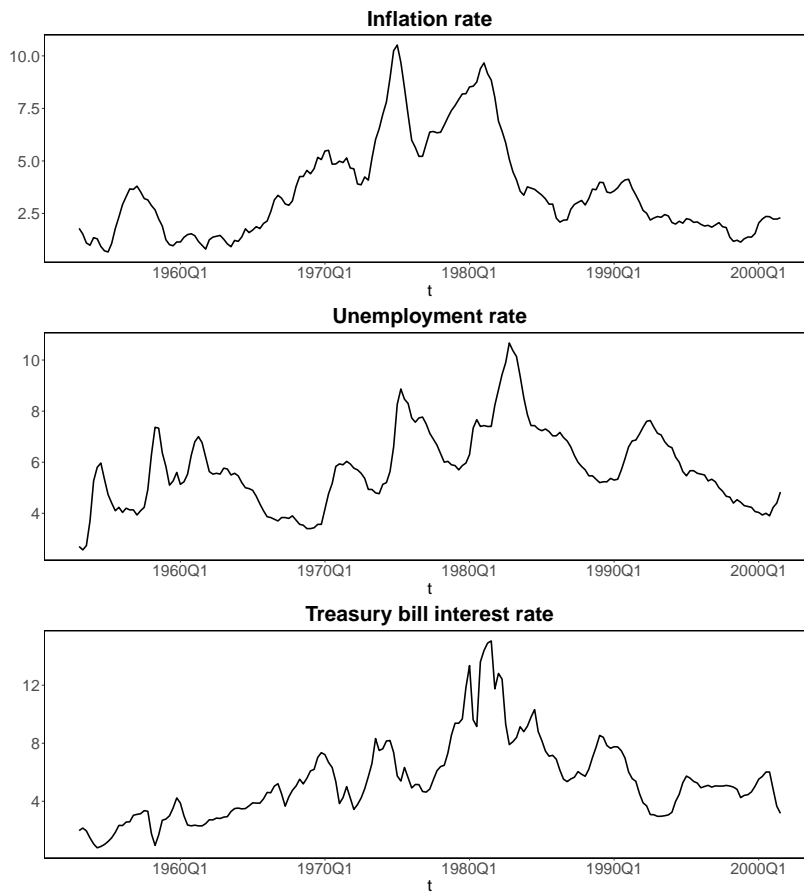


Figure 13. Inflation rate, unemployment rate and treasury bill interest rate for the US from 1953Q1 to 2001Q3

From Fig. 14, we can see that the estimated trends (red) for the first training sample ( $i = 1$ )

follow the observations (black) smoothly.

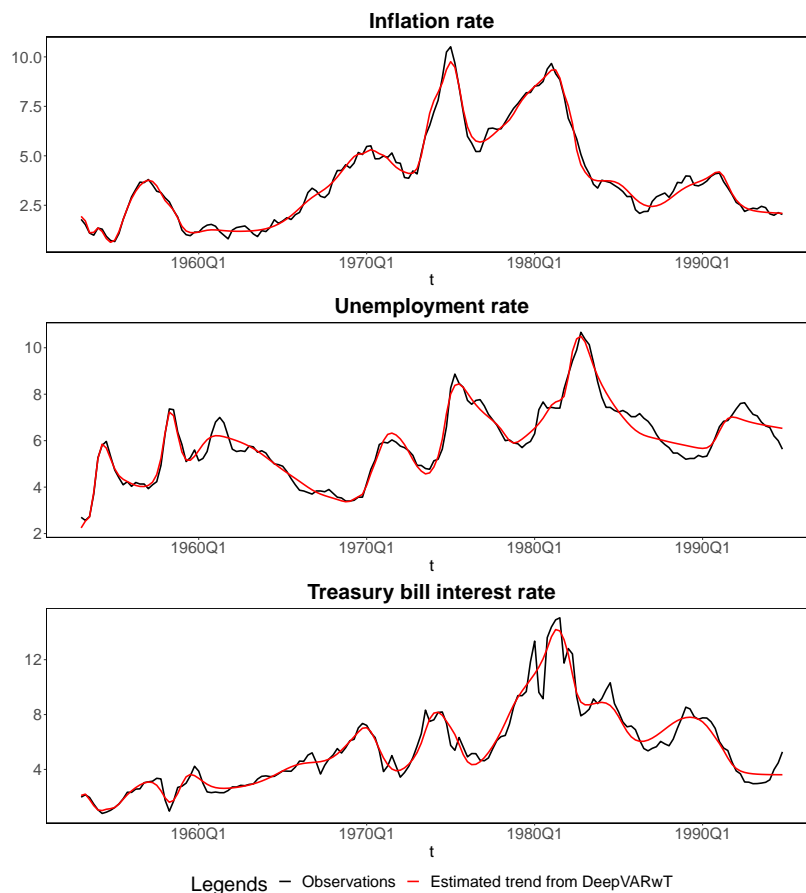


Figure 14. The first training sample (black lines) from 1953Q1 to 1994Q4 and the corresponding estimated trends (red lines).

The sample autocorrelations of residuals are shown in Fig. 15. The results are reasonably good for the inflation rate and treasury bill interest series, and a little concerning for the unemployment rate series in terms of the number of values outside the boundaries.

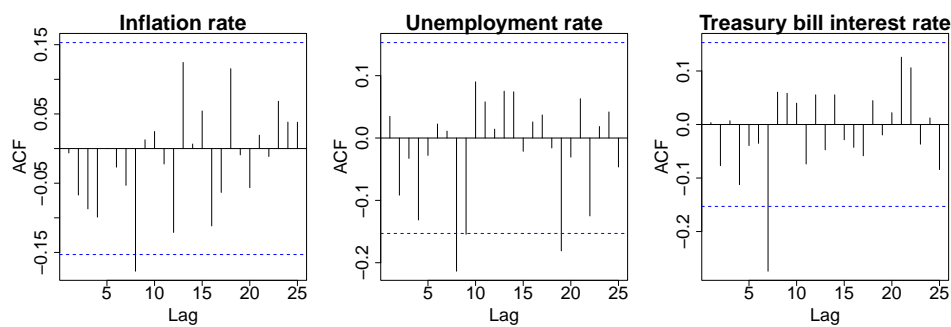


Figure 15. Sample autocorrelations of residuals.

Fig. 12 contains normal QQ plots of the residuals. There is some deviation from normality for all the series at both ends.



Figure 16. Normal QQ plots of residuals.

Table 4 shows the APE and SIS values of different models at several horizons  $h = 1, 2, 4, 8$  and averaged over  $h = 1 : 4$  and  $h = 1 : 8$ .

- **DeepVARwT vs VARwT.** Compared with the time-invariant VAR with trend, DeepT-VARwT produced better point forecasts at almost all forecasting horizons for all the series (except  $h = 1$  for inflation rate and  $h = 1, 2$  for treasury bill interest rate). It also gave more accurate prediction intervals at almost all forecasting horizons for all the series (except  $h = 1, 2$  for inflation rate).
- **DeepTVARwT vs other deep learning based models.** Compared with DeepAR and DeepState, our model produced more accurate point forecasts at almost all forecasting horizons for unemployment rate (except  $h = 1$ ) and treasury bill interest rate (except  $h = 1, 2$ ). Our model resulted in better prediction intervals at all forecasting horizons for unemployment rate and treasury bill interest rate.

Table 5. Performance of DeepVARwT against other models according to APE and SIS.

	Inflation rate											
	Absolute Percentage Error						Scaled Interval Score					
	$h=1$	$h=2$	$h=4$	$h=8$	$h=1:4$	$h=1:8$	$h=1$	$h=2$	$h=4$	$h=8$	$h=1:4$	$h=1:8$
VARwT	9.961	24.991	76.114	259.015	39.129	111.141	<b>1.281</b>	<b>2.388</b>	14.168	139.702	5.851	42.729
DeepAR	<b>7.763</b>	<b>15.281</b>	<b>28.017</b>	52.398	<b>18.497</b>	31.416	1.503	3.558	9.151	19.145	<b>5.164</b>	10.601
DeepState	18.373	22.375	29.036	40.723	24.191	31.294	5.388	7.947	10.443	14.500	8.176	11.139
DeepVARwT	13.707	24.019	34.797	<b>34.283</b>	25.646	<b>29.747</b>	1.882	4.626	<b>9.150</b>	<b>10.918</b>	5.553	<b>7.926</b>

	Unemployment rate											
	Absolute Percentage Error						Scaled Interval Score					
	$h=1$	$h=2$	$h=4$	$h=8$	$h=1:4$	$h=1:8$	$h=1$	$h=2$	$h=4$	$h=8$	$h=1:4$	$h=1:8$
VARwT	3.514	8.960	25.229	93.339	13.425	38.390	1.263	2.738	15.992	139.895	6.323	45.909
DeepAR	<b>3.250</b>	6.524	13.014	31.405	8.099	16.310	1.273	2.965	8.727	21.958	4.659	10.335
DeepState	15.144	15.941	19.629	25.726	17.515	20.596	6.292	9.277	11.428	15.207	9.676	12.328
DeepVARwT	3.447	<b>5.845</b>	<b>9.833</b>	<b>17.266</b>	<b>6.788</b>	<b>10.656</b>	<b>1.239</b>	<b>2.239</b>	<b>5.177</b>	<b>13.059</b>	<b>2.946</b>	<b>6.176</b>

	Treasury bill interest rate											
	Absolute Percentage Error						Scaled Interval Score					
	$h=1$	$h=2$	$h=4$	$h=8$	$h=1:4$	$h=1:8$	$h=1$	$h=2$	$h=4$	$h=8$	$h=1:4$	$h=1:8$
VARwT	5.390	10.537	20.041	75.861	12.581	30.385	2.110	3.211	4.875	44.500	3.452	13.042
DeepAR	<b>4.868</b>	<b>10.073</b>	18.693	24.993	12.340	18.016	1.583	3.904	13.264	18.202	6.848	12.436
DeepState	13.149	13.452	14.818	22.711	13.881	16.394	3.138	3.858	5.346	10.140	4.192	6.175
DeepVARwT	7.024	11.045	<b>11.688</b>	<b>16.699</b>	<b>10.130</b>	<b>12.626</b>	<b>1.409</b>	<b>2.728</b>	<b>3.045</b>	<b>4.048</b>	<b>2.444</b>	<b>3.234</b>

Over  $h = 1 : 4$  and  $h = 1 : 8$ , the DeepVARwT model outperformed other models in providing better forecasts and prediction intervals, except for the inflation rate over  $h=1:4$  where DeepAR did better.

The number of weight parameters in the network for the 20 fitted DeepVARwT models varied between 849 and 1350. The computation time for generating 20 predictions using VARwT, DeepAR, DeepState and DeepVARwT was about 1, 45, 80, and 59 minutes, respectively.

## 5. Summary and further discussion

In this work, we proposed a new approach to VAR modeling and forecasting by generating trends as well as model parameters using an LSTM network and the associated deep learning methodology for exact maximum likelihood estimation. A simulation study demonstrated the effectiveness of the proposed approach. Three examples with real data are provided to show that it competes well with existing models in terms of prediction performance.

Default values of the hyper-parameters for the DeepAR and DeepState models were used, which worked reasonably well but can be tweaked for better performance. The python code and data to reproduce forecasting results is available at <https://github.com/lixiobj/DeepVARwT-data-code>.

The computation becomes more challenging as the number/length of the component series increases. With high dimensional time series, a potential avenue for future research involves incorporating regularization and low-rank structure into the model fitting. One approach is to impose a low-rank assumption on  $A_1, \dots, A_p$  combined into a single matrix. This enables a reduction along one specific direction [27]. Building on this concept, [27] further rearranged  $A_i, i = 1, \dots, p$  into a tensor to reduce the dimension along three directions, allowing each direction to have a different low-rank structure. Incorporating a tensor structure into our DeepVARwT model could be a potential future direction.

The model that has been explored so far rely on the assumption of Gaussianity. However, in practical applications such as demand forecasting, series may exhibit sporadic occurrences with periods of no activity at all. This intermittent behaviour of demand calls for the relaxation of the Gaussian assumption to accommodate discrete data. It might be possible to generalise the digitised Gaussian ARMA model of [16] to the multivariate case.

## Acknowledgements

The first author's work was supported by The University of Manchester under a Dean's Doctoral Scholarship Award.

## Disclosure statement

No potential conflict of interest was reported by the authors.

## References

- [1] C.F. Ansley and R. Kohn, *A note on reparameterizing a vector autoregressive moving average model to enforce stationarity*, Journal of Statistical Computation and Simulation 24 (1986), pp. 99–106.
- [2] O. Barndorff-Nielsen and G. Schou, *On the parametrization of autoregressive models by partial autocorrelations*, Journal of Multivariate Analysis 3 (1973), pp. 408–419.
- [3] J. Duchi, E. Hazan, and Y. Singer, *Adaptive subgradient methods for online learning and stochastic optimization.*, Journal of Machine Learning Research 12 (2011).
- [4] J. Fan, Q. Yao, and Z. Cai, *Adaptive varying-coefficient linear models*, Journal of the Royal Statistical Society: Series B (Statistical Methodology) 65 (2003), pp. 57–80.
- [5] F.A. Gers, J. Schmidhuber, and F. Cummins, *Learning to forget: Continual prediction with LSTM*, Neural Computation 12 (2000), pp. 2451–2471.
- [6] T. Gneiting and A.E. Raftery, *Strictly proper scoring rules, prediction, and estimation*, Journal of the American Statistical Association 102 (2007), pp. 359–378.

- [7] E.J. Hannan, *Multiple time series*, Vol. 38, John Wiley & Sons, 1970.
- [8] D.I. Harvey and T.C. Mills, *Modelling global temperature trends using cointegration and smooth transitions*, *Statistical Modelling* 1 (2001), pp. 143–159.
- [9] S.E. Heaps, *Enforcing stationarity through the prior in vector autoregressions*, *Journal of Computational and Graphical Statistics* (2022), pp. 1–24.
- [10] S.E. Heaps, *Enforcing stationarity through the prior in vector autoregressions*, *Journal of Computational and Graphical Statistics* 32 (2023), pp. 74–83.
- [11] M.T. Holt and T. Teräsvirta, *Global hemispheric temperatures and co-shifting: A vector shifting-mean autoregressive analysis*, *Journal of Econometrics* 214 (2020), pp. 198–215.
- [12] M.A. Ivanov and S.N. Evtimov, *1963: The break point of the northern hemisphere temperature trend during the twentieth century*, *International Journal of Climatology* 30 (2010), pp. 1738–1746.
- [13] Ò. Jordà, *Estimation and inference of impulse responses by local projections*, *American Economic Review* 95 (2005), pp. 161–182.
- [14] G. Koop, D. Korobilis, et al., *Bayesian multivariate time series methods for empirical macroeconomics*, *Foundations and Trends® in Econometrics* 3 (2010), pp. 267–358.
- [15] G.M. Koop, *Forecasting with medium and large Bayesian VARs*, *Journal of Applied Econometrics* 28 (2013), pp. 177–203.
- [16] H. Lennon and J. Yuan, *Estimation of a digitised Gaussian ARMA model by Monte Carlo expectation maximisation*, *Computational Statistics & Data Analysis* 133 (2019), pp. 277–284.
- [17] H. Lütkepohl, *New introduction to multiple time series analysis*, Springer Science & Business Media, 2005.
- [18] M. Morf, A. Vieira, T. Kailath, et al., *Covariance characterization by partial autocorrelation matrices*, *The Annals of Statistics* 6 (1978), pp. 643–648.
- [19] C.P. Morice, J.J. Kennedy, N.A. Rayner, and P.D. Jones, *Quantifying uncertainties in global and regional temperature change using an ensemble of observational estimates: The HadCRUT4 data set*, *Journal of Geophysical Research: Atmospheres* 117 (2012).
- [20] A. Paszke, S. Gross, F. Massa, A. Lerer, J. Bradbury, G. Chanan, T. Killeen, Z. Lin, N. Gimelshein, L. Antiga, A. Desmaison, A. Kopf, E. Yang, Z. DeVito, M. Raison, A. Tejani, S. Chilamkurthy, B. Steiner, L. Fang, J. Bai, and S. Chintala, *Pytorch: An imperative style, high-performance deep learning library*, in *Advances in Neural Information Processing Systems* 32, H. Wallach, H. Larochelle, A. Beygelzimer, F. d'Alché-Buc, E. Fox, and R. Garnett, eds., Curran Associates, Inc., 2019, pp. 8024–8035. Available at <http://papers.neurips.cc/paper/9015-pytorch-an-imperative-style-high-performance-deep-learning-library.pdf>.
- [21] B. Pfaff and M. Stigler, *vars: VAR Modelling* (2018). Available at <https://cran.r-project.org/web/packages/vars/index.html>, R package version 1.5-3.
- [22] G.E. Primiceri, *Time varying structural vector autoregressions and monetary policy*, *The Review of Economic Studies* 72 (2005), pp. 821–852.
- [23] S.S. Rangapuram, M.W. Seeger, J. Gasthaus, L. Stella, Y. Wang, and T. Januschowski, *Deep state space models for time series forecasting*, in *Advances in Neural Information Processing Systems*. 2018, pp. 7785–7794.
- [24] A. Roy, T.S. McElroy, and P. Linton, *Constrained estimation of causal invertible VARMA*, *Statistica Sinica* 29 (2019), pp. 455–478.
- [25] D. Salinas, V. Flunkert, J. Gasthaus, and T. Januschowski, *DeepAR: Probabilistic forecasting with autoregressive recurrent networks*, *International Journal of Forecasting* 36 (2020), pp. 1181–1191.
- [26] M.P. Wand and M.C. Jones, *Kernel smoothing*, CRC Press, 1994.
- [27] D. Wang, Y. Zheng, H. Lian, and G. Li, *High-dimensional vector autoregressive time series modeling via tensor decomposition*, *Journal of the American Statistical Association* 117 (2022), pp. 1338–1356.
- [28] Y. Wang, A. Smola, D. Maddix, J. Gasthaus, D. Foster, and T. Januschowski, *Deep factors for forecasting*, in *International Conference on Machine Learning*. PMLR, 2019, pp. 6607–6617.

## Appendix A. Prediction error variances and covariances

First consider the model for  $\{\mathbf{y}_t\}$  to be VAR(1) with trend:

$$\mathbf{y}_t - \boldsymbol{\mu}_t = A(\mathbf{y}_{t-1} - \boldsymbol{\mu}_{t-1}) + \boldsymbol{\varepsilon}_t, \quad (\text{A1})$$

where  $\{\boldsymbol{\varepsilon}_t\}$  is white noise,  $\boldsymbol{\varepsilon}_t \sim \mathcal{N}(\mathbf{0}, \Sigma)$  and  $\boldsymbol{\varepsilon}_t$  is uncorrelated with  $\mathbf{y}_{t-1}, \mathbf{y}_{t-2}, \dots$

Then, we can decompose  $\mathbf{y}_{T+\ell}$  starting with  $\mathbf{y}_T$  for  $\ell = 1, \dots, h$ :

$$\begin{aligned} \mathbf{y}_{T+1} - \boldsymbol{\mu}_{T+1} &= A(\mathbf{y}_T - \boldsymbol{\mu}_T) + \boldsymbol{\varepsilon}_{T+1}, \\ \mathbf{y}_{T+2} - \boldsymbol{\mu}_{T+2} &= A(\mathbf{y}_{T+1} - \boldsymbol{\mu}_{T+1}) + \boldsymbol{\varepsilon}_{T+2} = A^2(\mathbf{y}_T - \boldsymbol{\mu}_T) + A\boldsymbol{\varepsilon}_{T+1} + \boldsymbol{\varepsilon}_{T+2}, \\ \mathbf{y}_{T+3} - \boldsymbol{\mu}_{T+3} &= A^3(\mathbf{y}_T - \boldsymbol{\mu}_T) + A^2\boldsymbol{\varepsilon}_{T+1} + A\boldsymbol{\varepsilon}_{T+2} + \boldsymbol{\varepsilon}_{T+3}, \\ &\vdots \\ \mathbf{y}_{T+h} - \boldsymbol{\mu}_{T+h} &= A^h(\mathbf{y}_T - \boldsymbol{\mu}_T) + \sum_{i=0}^{h-1} A^i \boldsymbol{\varepsilon}_{T+h-i}, \end{aligned} \quad (\text{A2})$$

where  $A^i$  is understood to be the identity matrix when  $i = 0$ .

From (A2), the best linear predictor for  $\mathbf{y}_{T+\ell}$  given  $\mathbf{y}_T, \mathbf{y}_{T-1}, \dots$  is

$$\hat{\mathbf{y}}_{T+\ell} = E[\mathbf{y}_{T+\ell} | \mathbf{y}_T, \mathbf{y}_{T-1}, \dots] = A^\ell(\mathbf{y}_T - \boldsymbol{\mu}_T) + \boldsymbol{\mu}_{T+\ell}, \quad (\text{A3})$$

and the associated prediction error variance-covariance matrix is

$$\text{Var}\{\mathbf{y}_{T+\ell} - \hat{\mathbf{y}}_{T+\ell}\} = \sum_{i=0}^{\ell-1} A^i \Sigma (A^i)'. \quad (\text{A4})$$

When  $\{\mathbf{y}_t\}$  follows the VAR( $p$ ) model (3) with trend, we use its VAR(1) form

$$\mathbf{y}_t^* - \boldsymbol{\mu}_t^* = A^*(\mathbf{y}_{t-1}^* - \boldsymbol{\mu}_{t-1}^*) + \boldsymbol{\varepsilon}_t^*, \quad (\text{A5})$$

where  $\mathbf{y}_t^* = (\mathbf{y}'_t, \mathbf{y}'_{t-1}, \dots, \mathbf{y}'_{t-p+1})'$ ,  $\boldsymbol{\mu}_t^* = (\boldsymbol{\mu}'_t, \boldsymbol{\mu}'_{t-1}, \dots, \boldsymbol{\mu}'_{t-p+1})'$ ,

$$A^* = \begin{bmatrix} A_1 & A_2 & \cdots & \cdots & A_p \\ I & \mathbf{0} & \cdots & \cdots & \mathbf{0} \\ \mathbf{0} & I & \ddots & & \vdots \\ \vdots & \ddots & \ddots & \ddots & \vdots \\ \mathbf{0} & \cdots & \mathbf{0} & I & \mathbf{0} \end{bmatrix}, \quad (\text{A6})$$

and

$$\mathbf{y}_t = [I, \mathbf{0}, \dots, \mathbf{0}]\mathbf{y}_t^*. \quad (\text{A7})$$

The variance-covariance matrix of  $\boldsymbol{\varepsilon}_t^* = (\varepsilon_t', \mathbf{0}', \dots, \mathbf{0}')$  is

$$\Sigma^* = \begin{bmatrix} \Sigma & \mathbf{0} \\ \mathbf{0} & \mathbf{0} \end{bmatrix}. \quad (\text{A8})$$

Using (A3), the best linear predictor for  $\mathbf{y}_{t+h}^*$  given  $\mathbf{y}_t^*, \mathbf{y}_{t-1}^*, \dots$  is

$$\hat{\mathbf{y}}_{t+h}^* = (A^*)^h (\mathbf{y}_t^* - \boldsymbol{\mu}_t^*) + \boldsymbol{\mu}_{t+h}^*. \quad (\text{A9})$$

Using (A4), the variance-covariance matrix of the prediction error for  $\hat{\mathbf{y}}_{t+h}^*$  is

$$\sum_{i=0}^{h-1} (A^*)^i \Sigma^* ((A^*)^i)'. \quad (\text{A10})$$

The prediction for  $\mathbf{y}_{t+h}$  can be extracted from that for  $\mathbf{y}_{t+h}^*$ . The prediction error variance-covariance matrix for  $\hat{\mathbf{y}}_{t+h}$  is in the top-left corner of the above.